Molecular Crystals and Liquid Crystals
Publication details, including instructions for authors and subscription information:
http://www.tandfonline.com/loi/gmcl20

Development of Efficient Organic Solar Cells Based on Triarylamine-Functionalized Ruthenium Dyes

Yoshinori Nishikitani [a], Takaya Kubo [a b] & Hideki Masuda [c]

[a] Central Technical Research Laboratory, Research & Development Division, JX Nippon Oil & Energy Corporation, Yokohama, Japan

[b] Research Center for Advanced Science and Technology, University of Tokyo, Tokyo, Japan

[c] Department of Applied Chemistry, Graduate School of Engineering, Nagoya Institute of Technology, Nagoya, Japan

Version of record first published: 16 May 2011

To cite this article: Yoshinori Nishikitani, Takaya Kubo & Hideki Masuda (2011): Development of Efficient Organic Solar Cells Based on Triarylamine-Functionalized Ruthenium Dyes, Molecular Crystals and Liquid Crystals, 538:1, 1-9

To link to this article: http://dx.doi.org/10.1080/15421406.2011.563205

Mol. Cryst. Liq. Cryst., Vol. 538: pp. 1–9, 2011

ISSN: 1542-1406 print/1563-5287 online
DOI: 10.1080/15421406.2011.563205

Taylor & Francis
Taylor & Francis Group

Development of Efficient Organic Solar Cells Based on Triarylamine-Functionalized Ruthenium Dyes

YOSHINORI NISHIKITANI,[1] TAKAYA KUBO,[1,2] AND HIDEKI MASUDA[3]

[1]Central Technical Research Laboratory, Research & Development Division, JX Nippon Oil & Energy Corporation, Yokohama, Japan
[2]Research Center for Advanced Science and Technology, University of Tokyo, Tokyo, Japan
[3]Department of Applied Chemistry, Graduate School of Engineering, Nagoya Institute of Technology, Nagoya, Japan

New materials and structures have been developed for efficient organic solar cells such as dye-sensitized solar cells (DCSs) and organic thin-film solar cells (OPVs). In this paper, the authors discuss various strategies for achieving high conversion efficiency in organic solar cells, focusing on nanostructured materials. In the case of DSCs, TiO_2 nanotubes with suitable dimensions are expected to function as efficient charge transport layers because the rate constant of back electron transfer in a TiO_2 nanotube layer is smaller than that in a nanoparticule layer. A new derivative of triarylamine-functionalized ruthenium dyes is also synthesized, aimed at the efficient electron transfer from the dye to TiO_2. Furthermore, OPVs based on donor/acceptor (D/A) block copolymers are discussed, focusing on the exciton binding energy of donor and acceptor segments.

Keywords Donor/acceptor (D/A) block copolymers; dye-sensitized solar cells; exciton binding energy; organic thin-film solar cells; TiO_2 nanotubes; triarylamine-functionalized ruthenium dyes

Introduction

Organic solar cells have received considerable attention due to their great potential for low-cost, flexible and light-weight photovoltaic devices. Organic solar cells are classified into two types: so-called Grätzel type dye-sensitized solar cells (DSCs) [1]; and organic thin-film solar cells (OPVs) [2–4]. Due to great progress in increasing the conversion efficiency of DSCs, efficiency of up to around 11% has been reported [5], which compares favorably with amorphous silicon-based solar cells. Further effort is necessary to increase the conversion efficiency and improve durability for

Address correspondence to Yoshinori Nishikitani, Central Technical Research Laboratory, Research & Development Division, JX Nippon Oil & Energy Corporation, 8 Chidori-cho, Naka-ku, Yokohama 231-0815, Japan. Tel.: +81-45-625-7179; Fax: +81-45-625-7298; E-mail: yoshinori.nishikitani@noe.jx-group.co.jp

outdoor applications. Work is underway to develop new dyes which absorb longer-wavelength light and/or yield higher molar extinction coefficients, to further improve light-harvesting efficiencies [6–8]. The solidification or quasi-solidification of the electrolyte solution is one way to improve cell durability by preventing the leakage of the electrolyte solution in DSCs [9–13]. We previously reported on our work with quasi-solid state DSCs using gel-type, ionically conductive polymers (ICPs) based on poly(vinylidenefluoride-*co*-hexafluoropropylene) (PVDF-HFP) to reduce the leakage of the electrolyte solution [10]. Aimed at increasing DSC conversion efficiency, we have also developed two key materials: (1) ultrahigh-aspect-ratio TiO_2 nanotubes made by anodic oxidation of Ti metals in extremely dilute perchloric acid solution, to establish good carrier pathways [14–16]; and (2) novel triarylamine-functionalized ruthenium dyes, to harvest sunlight efficiently [17–19]. DSCs with the TiO_2 nanotubes (TNT) were found to provide higher light-harvesting efficiencies than conventional DSCs with TiO_2 nanoparticle (NP) photoanodes [20,21]. Several different triarylamine-functionalized ruthenium dyes were synthesized to achieve efficient electron injection from the dye to the TiO_2 as well as faster regeneration of the cationic dye.

OPVs are solid-state photovoltaic devices using organic semiconductors, usually employing bulk-heterojunction structures made up of interpenetrating donor and acceptor materials, which successfully achieves efficient exciton dissociation to create free carriers, thereby increasing the conversion efficiency [22–24]. One of the recent research subjects with regard to OPVs is finding a way of providing not only a large charge separation interface, but also good carrier pathways to increase carrier collection efficiency. Donor/acceptor (D/A) block copolymers have also been proposed for bulk-heterojunction organic thin-film solar cells, aimed at establishing self-organized well-ordered donor/acceptor nanophase separation [25,26]. Our numerical simulations showed that the HOMO and LUMO energy levels and segment lengths of the donor and acceptor blocks were key parameters, and also indicated that conversion efficiency would be higher if each D/A segment length were designed to be shorter than the respective exciton diffusion length.

In this manuscript, discussed are various strategies for achieving high photon-to-electricity conversion efficiency in these solar cells, focusing on solar cell structures as shown in Figure 1. In the case of DSCs, unlike NPs, TNTs with suitable dimensions are expected to function as efficient carrier transport layer as well as to give large surface areas for charge separation. Furthermore, OPVs based on donor/acceptor (D/A) block copolymers are discussed, focusing on the phase separation of donor and acceptor segments and exciton binding energy in their segments.

Methods

Fabrication of Dye-Sensitized Solar Cells. Two different types of TiO_2 photoanodes were prepared. The photoanode with TNTs is formed as follows [14]: A TNT powder synthesized by anodizing a Ti sheet ($5 \times 10\,cm^2$, 0.5 mm thick) in a $0.1\,mol \cdot L^{-1}$ perchloric acid solution; and a TNT powder, which was rinsed with water and dried in air, were dispersed in *tert*-butyl alcohol, which was used as an electrolyte for electrophoretic deposition (EPD). A fluorine-doped SnO_2 transparent conducting oxide (FTO) substrate and the counter electrode were held together with a gap of 1.0 mm by placing a 1.0 mm-thick and 2.0 mm-wide silicone spacer film on the three peripheral sides, leaving the uppermost side open for injecting the TNT

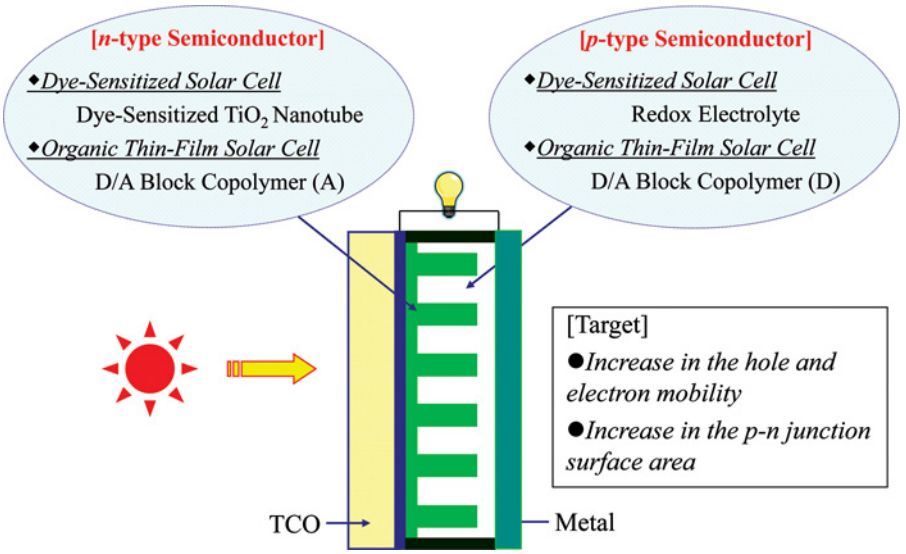

Figure 1. Targeting structure of organic solar cells.

dispersed *tert*-butyl alcohol. The TNT layer (about 10 μm) was deposited on the FTO substrate by applying a DC electric field of $-1000\,V \cdot cm^{-1}$ for 3 minutes. The TNT layer was then annealed at 723 K for 1 hour. Transparent NP layers (Ti Nanoxide-T, Solaronix) with a thickness of about 10 μm were formed on FTO glass substrates ($15\,\Omega \cdot sq^{-1}$, TEC15) by the doctor-blade method. The NP layers were annealed at 723 K for 1 hour.

Photoanodes were formed by immersing the TiO_2-layers formed on FTO substrates in a mixed solution of *tert*-butyl alcohol and DMF (volume ratio: 1:1) containing 0.5 mM dye (Ruthenium-535-bis-TBA (N719), Solaronix) and 0.05 M deoxycholic acid (DCA) at room temperature for 3 hours. DSCs were fabricated by assembling a photoelectrode and Pt-counter electrode with a hot-melt ionomer film as a spacer placed between the electrodes. The cell gap between the FTO substrate and counter electrodes was about 23 μm. An electrolyte solution (0.50 M 2,3-dimethyl-1-propylimidazolium iodide (DMPII), 0.05 M I_2, 0.10 M LiI, 0.5 M *tert*-butylpyridine and 0.05 M deoxycholic acid (DCA) in acetonitrile) was injected to the cell through a hole drilled in the counter electrode of the assembled cell. Finally, the injection hole was sealed using a hot-melt ionomer film by heating.

Characterization and Measurements. The current-voltage (*J-V*) characteristics were measured at 296 K in a temperature-controlled chamber with a potentiostat (Schlumberger 1287 Solartron) under illumination (AM1.5, $100\,mW \cdot cm^{-2}$) using a solar simulator (YSS-150, Yamashita-Denso). The exposed area of all the cells was limited to $0.15\,cm^2$ by using a metal-mask.

Synthesis of J7. A mixture of [RuCl(N-(1,4-dimethoxyphenyl)-N-2-pyridinyl-2-pyridinamine)(*p*-cymene)]Cl and 4,4′-bis(carboxyvinyl)-2,2′-bipyridine in 30 ml of dry DMF was heated at 140°C under Ar for 4 hours in the dark. NH_4NCS was then added to the mixture and treated at 140°C for 4 hours. After cooling to room temperature, the DMF was evaporated and water was added. The resulting

purple solid was filtered and washed with water. The crude complex was dissolved in basic methanol with tetrabutylammonium hydroxide (TBAOH) and further purified on a Sephadex LH-20 column using methanol as the eluent.

Results and Discussion

Dye-sensitized solar cells. Improvement of the charge collection efficiency at the electrode by achieving faster electron-transport in TiO_2 layers and slower electron recombination with cationic dyes and/or redox species is very important to increase the conversion efficiency of DSCs. From this viewpoint, TNTs are becoming increasingly important in DSC technology since there is a potential for providing good electron transport pathways.

Table 1 shows *J-V* characteristics of two different DSCs fabricated with TNTs or NPs. Two different *J-V* curves were measured on each cell by illuminating it, respectively, from the front-side and back-side. V_{oc}s of TNT-based DSCs were turned out to be higher than those of NP-based DSCs in both illumination conditions.

The open-circuit voltage of the cell is expressed as follows [27]:

$$V_{oc} = \frac{kT}{qu\alpha} \ln\left(\frac{AI_0}{n_0^{u\alpha} k_{et} c_{ox}^m}\right) \tag{1}$$

where k is the Boltzmann constant, q is the electric charge, u and m are the order of the rate of reaction, respectively, for oxidized redox species and electron, α is the electron-transfer coefficient, I_0 is the incident photon flux, A is the ratio of adsorbed photon flux to I_0, k_{et} is the rate constant for back electron transfer, n_0 is the electron population in semiconductor in the dark, and c_{ox} is the concentration of oxidized redox species. Since the reaction orders *u, m* and the electron transfer coefficient α can be effectively taken as unity, V_{oc} can be then expressed in a simpler form as follows:

$$V_{oc} = \frac{kT}{q} \ln\left(\frac{AI_0}{n_0 k_{et} c_{ox}}\right) \tag{2}$$

From Eq. (2), the back-electron-transfer rate constant k_{et} is derived;

$$k_{et} = \frac{AI_0}{n_o c_{ox}} \exp\left(-\frac{qV_{OC}}{kT}\right) \tag{3}$$

Table 1. *J-V* characteristics of dye-sensitized solar cells fabricated with TNT and NP

TiO_2	J_{sc} mA · cm^{-2}	V_{oc} V	*FF*	Efficiency %	Illumination
TNT	10.3	0.744	0.736	5.64	Front-side
NP	11.0	0.729	0.731	5.88	Front-side
TNT	10.1	0.806	0.645	5.27	Back-side
NP	7.1	0.764	0.631	3.14	Back-side

Therefore, the ratio of the back-electron-transfer rate constants of k_{et}^{TNT} in TNT-based DSCs and k_{et}^{NP} in NP-based DCSs is obtained as follows:

$$\frac{k_{et}^{NP}}{k_{et}^{TNT}} = \exp\left\{-\frac{q}{kT}(V_{OC}^{NP} - V_{OC}^{TNT})\right\} \tag{4}$$

The ratio of the back-electron-transfer rate constants in Eq. (4) is calculated with the open-circuit voltage values given in Table 1. The back-electron-transfer rate constant k_{et}^{TNT} was found out to be 1.8 times slower than k_{et}^{NP} in the case of front-side illumination, while the rate constant became 5.1 times slower than k_{et}^{NP} in the case of back-side illumination. Similar results were reported on TNT array-based DSCs wherein TNT arrays were prepared by electrochemically anodizing Ti foils in NH_4F electrolyte [20]. These facts indicate that the charge collection efficiency is markedly increased by employing one-dimensional TiO_2 nano-materials.

We have developed novel triarylamine-functionalized ruthenium dyes (**J5** and **J6**) as sensitizers for DSCs, and reported photovoltaic performance of the DSCs previously (Table 2). The introduction of electron donating groups such as alkoxy and amine groups on the triarylamine-ancillary ligand provided directionality to the efficient electron transfer from the dye to TiO_2. Among the dyes sensitized (**J5** and **J6**), **J6** bearing a methoxy group substituent to the phenyl ring (Fig. 2) gives the best performance as a sensitizer [17]. Here, we synthesized a novel triarylamine-functionalized ruthenium dye, **J7**, having two methoxy groups, to study the effect of electron donating properties of the dyes on solar cell performances, aimed at gaining insight into obtaining higher efficiency triarylamine-functionalized ruthenium-dyes.

Figure 3 shows absorption spectra of **J6** and **J7** in *N,N*-dimethyl formamide (DMF) solution. The absorption spectra of **J6** and **J7** are quite similar to each other in their spectral shapes, indicating that addition of one more methoxy group to phenyl ring has little effect on absorption characteristics. The IPCE spectra of the DSCs with two different photoanodes sensitized, respectively, with **J6** and **J7** start to increase at about 850 nm and reach a maximum value of about 80% around 550 nm. The DFT calculation on the dyes of **J6** and **J7** verified that both dyes have HOMO and LUMO levels at almost same energy: the HOMO and LUMO of **J6** are −5.17 eV and −2.88 eV, and the HOMO and LUMO of **J7** are −5.15 eV and −2.87 eV, respectively. Compared with the performance of the DSCs with the dye of **J5**, which bears no methoxy groups on the triarylamine-ancillary ligand, the introduction of methoxy groups on the triarylamine-ancillary ligand was confirmed to provide directionality to the efficient electron transfer from the dye to TiO_2, thereby increasing solar cell performances such as conversion efficiency and IPCE values.

Table 2. *J-V* characteristics of dye-sensitized solar cells fabricated with different dyes

Dye	J_{sc} mA · cm^{-2}	V_{oc} V	*FF*	Efficiency %
J5	0.58	14.1	0.71	5.8
J6	0.63	17.9	0.70	7.9
J7	0.71	15.3	0.72	7.8

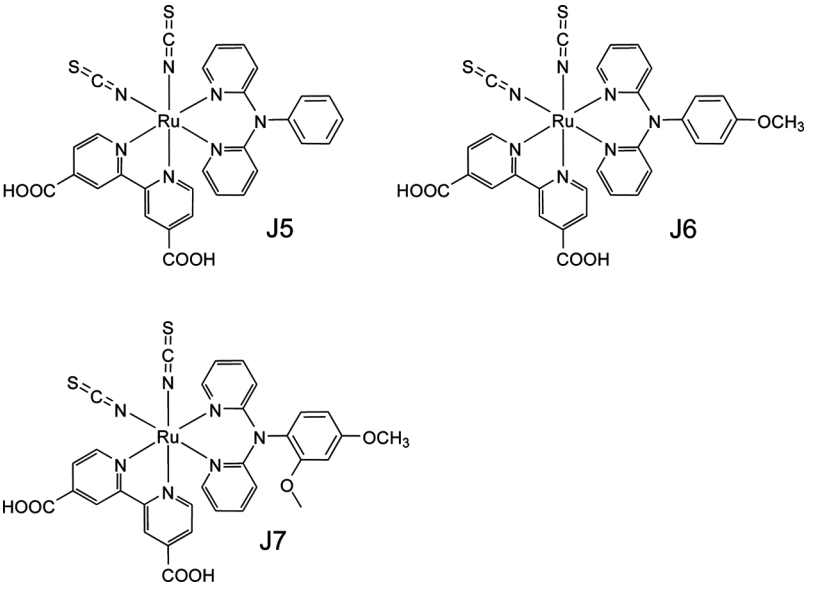

Figure 2. Molecular structures of **J5**, **J6** and **J7**.

Organic thin-film solar cells. It is reported that certain di-block copolymers form well-ordered nano-sized domain structures such as lamellas, cylinders or columns by the self-organization taking place under a suitable condition. In the case of D/A block copolymers designed for OPVs, phase-separated donor and acceptor segments formed by this self-organization are expected to provide well-ordered hole and electron transport layers, respectively. Here we will discuss optimal molecular structures for D/A block copolymers to achieve higher conversion efficiencies of OPVs fabricated with the block copolymers by focusing on the energy gap between the HOMO level of the donor and acceptor ($\delta E(HOMO)$) and that between the LUMO

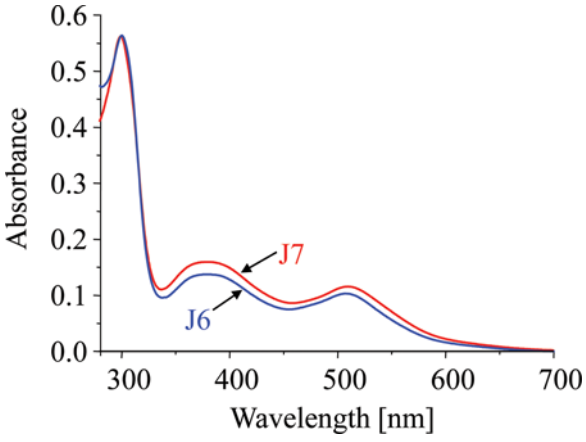

Figure 3. Absorption spectra of **J6** and **J7** measured in *N,N*-dimethylformamide (DMF) solution.

level of the donor and acceptor ($\delta E(LUMO)$) which closely relates to the efficiency of free carrier generation by exciton separation.

An optimal energy gap was estimated based on the assumption, for simplicity, that only the donor molecules absorb sunlight, and that the donor and acceptor domain sizes are the same. The conversion efficiency can be obtained by $\eta = J_{sc}V_{oc}FF$ where J_{sc} is the short-circuit current density, V_{oc} the open-circuit voltage, and FF the fill factor. If the band gap E_g (the energy difference between the HOMO and LUMO levels) of the donors, which closely relates with the light-harvesting efficiency, is assumed to be constant, the conversion efficiency is determined by the open-circuit voltage alone since J_{sc} is assumed to be constant. In this case, the open-circuit voltage V_{oc} is then given by Eq. (5) [28,29].

$$V_{oc} = (1/e)(E_g - \lambda_s - E_B) - 0.3V \tag{5}$$

where e is the elementary charge, λ_s is the Marcus reorganization energy, and E_B is the exciton binding energy. The exciton binding energy in organic semiconductors is given by the Coulomb repulsion energy U plus a small constant as shown in Eq. (6), and hence the open-circuit voltage can be expressed finally by Eq. (7) depending on the molecular shapes [30,31].

$$E_B \approx U + 0.1eV \tag{6}$$

$$V_{oc} = (1/e)(E_g - \lambda_s - U) - 0.4V \tag{7}$$

We assume that a molecules have a columnar structure as shown in Figure 4, where a is the diameter, l the length of a small columnar-segment, and n the number of columnar-segments. The column is composed of a small columnar-segment whose length is l. In this case, the equation of the open-circuit voltage V_{oc} is given by the following equation:

$$V_{oc} = (1/e)\left\{E_g - \lambda_s - \frac{e^2}{\pi\varepsilon_0\varepsilon_r nl}\ln\left(\frac{d}{a}\right)\right\} - 0.4V \tag{8}$$

where ε_0 is the vacuum permittivity, and ε_r the relative constant. Finally, Eq. (8) for the open-circuit voltage V_{oc} is rewritten in a simpler form of Eq. (9).

$$V_{oc} = V_{oc}^{*} - \frac{V^1}{n} \tag{9}$$

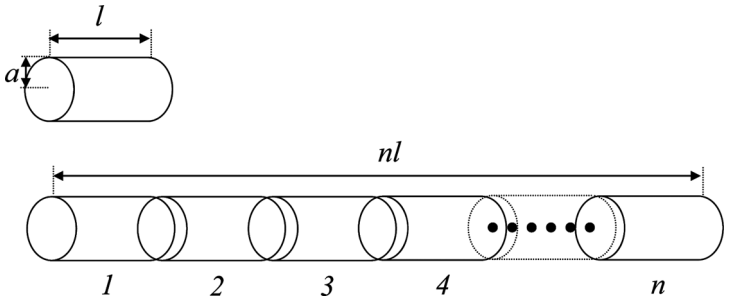

Figure 4. Models of molecular structures for calculating the exciton binding energy.

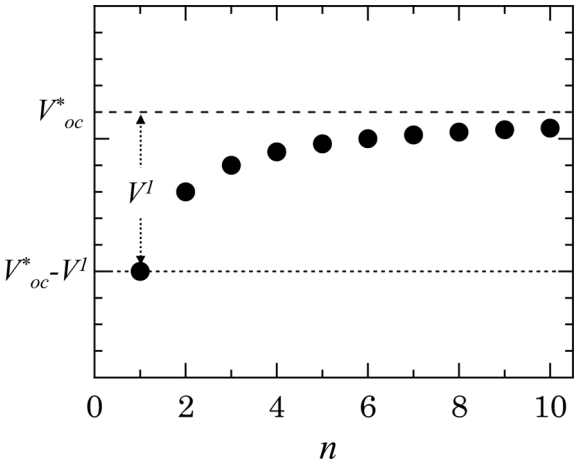

Figure 5. Dependence of V_{oc} on molecular structures.

$$V^*_{oc} = (1/e)(E_g - \lambda_s) - 0.4V \tag{10}$$

$$V^1 = \frac{e}{\pi\varepsilon_0\varepsilon_r l}\ln\left(\frac{d}{a}\right) \tag{11}$$

Here V^*_{oc} represents the open-circuit voltage of the cell based on an ideal molecule having an infinite chain length and V^1 represents the Coulomb repulsion energy of an individual small columnar-segment.

Figure 5 shows the dependence of V_{oc} on n obtained with Eq. (9). It indicates that the lager the D and/or A segments become the higher the V_{oc} gets. It means that the optimization of D/A segment structures corresponding to exction binding energy is crucial to achieving higher conversion efficiency.

Summary and Conclusions

In the case of DSCs, one-dimensional TiO_2 nanotubes with a high aspect ratio were expected to provide not only good light scatterers but also large charge separation areas, and to function as efficient charge transport layers because the rate constant of back electron transfer in TNT layer is smaller than that in NP layer. We then surmised that a DSC with a photoanode composed of optimally aligned TNTs would provide much higher photon-to-electricity conversion efficiency than the measured conversion efficiency values. To gain insight into the triarylamine-functionalized Ru-dye structures capable of producing high-efficiency DSCs, we studied the effect of methoxy ligands.

In the case of OPVs, the optimal donor and/or acceptor segment sizes were calculated with a model structure. The calculations indicate that larger donor and/or acceptor segments have smaller exciton binding energy and achieve even higher conversion efficiency in OPVs.

References

[1] O'Regan, B., & Grätzel, M. (1991). *Nature*, *353*, 737.
[2] Tang, C. W. (1986). *Appl. Phys. Lett.*, *48*, 183.
[3] Hiramoto, M., Fujiwara, H., & Yokoyama, M. (1991). *Appl. Phys. Lett.*, *58*, 1062.
[4] Sariciftci, N. S., Smilowitz, L., Heeger, A. J., & Wudl, F. (1992). *Science*, *258*, 1474.
[5] Green, M. A., Emery, K., Hishikawa, Y., & Warta, W. (2009). *Prog. Photovolt: Res. Appl.*, *17*, 320.
[6] Grätzel, M. (2008). *Bull. Jpn. Soc. Coord. Chem.*, *51*, 3.
[7] Altobello, S., Argazzi, R., Caramori, S., Contado, C., Da Fre, S., Rubino, P., Chone, C., Larramona, G., & Bignozzi, C. A. (2005). *J. Am. Chem. Soc.*, *127*, 15342.
[8] Dy, J. T., Tamaki, K., Sanehira, Y., Nakazaki, J., Uchida, S., Kubo, T., & Segawa, H. (2009). *Electrochemistry*, *77*, 206.
[9] Wang, P., Zakeeruddin, S. M., Moser, J. E., Nazeeruddin, M. K., Sekiguchi, T., & Grätzel, M. (2003). *Nature Materials*, *2*, 402.
[10] Asano, T., Kubo, T., & Nishikitani, Y. (2004). *J. Photochem. Photobiol. A Chemistry*, *164*, 111.
[11] Kubo, W., Kambe, S., Nakada, S., Kitamura, T., Hanabusa, K., Wada, Y., & Yanagida, S. (2003). *J. Phys. Chem. B*, *107*, 4374.
[12] Kim, J. H., Kang, M.-S., Kim, Y. J., Won, J., Park, N.-G., & Kang, Y. S. (2004). *Chem. Commun.*, 1662.
[13] Kato, T., Kado, T., Tanaka, S., Okazaki, A., & Hayase, S. (2006). *J. Electrochem. Soc.*, *153*, A626.
[14] Nakayama, K., Kubo, T., & Nishikitani, Y. (2008). *Jpn. J. Appl. Phys.*, *47*, 6610.
[15] Nakayama, K., Kubo, T., & Nishikitani, Y. (2008). *Appl. Phys. Exp.*, *1*, 112301.
[16] Nakayama, K., Kubo, T., & Nishikitani, Y. (2008). *Electrochem. Solid State Lett.*, *11*(3), C23.
[17] Jin, Z., Masuda, H., Yamanaka, N., Minami, M., Nakamura, T., & Nishikitani, Y. (2008). *Chem. Sus. Chem.*, *1*, 901.
[18] Jin, Z., Masuda, H., Yamanaka, N., Minami, M., Nakamura, T., & Nishikitani, Y. (2009). *J. Phys. Chem. C*, *113*, 2618.
[19] Jin, Z., Masuda, H., Yamanaka, N., Minami, M., Nakamura, T., & Nishikitani, Y. (2009). *Chem. Lett.*, *38*(1), 44.
[20] Zhu, K., Neale, N. R., Miedaner, A., & Frank, A. J. (2007). *Nano Lett.*, *7*, 69.
[21] Wang, Q., Zhu, K., Neale, N. R., & Frank, A. J. (2009). *Ibid.*, *9*, 806.
[22] Hiramoto, M., Fujiwara, H., & Yokoyama, M. (1991). *Appl. Phys. Lett.*, *58*, 1062.
[23] Yu, G., Gao, J., Hummelen, J. C., Wudl, F., & Heeger, A. J. (1995). *Science*, *270*, 1789.
[24] Nishikitani, Y., Uchida, S., & Kubo, T. (2006). *Nanostructured Materials for Solar Energy Conversion*, Soga, T. (Eds.), Elsevier Science Publisher: Amsterdam, Chapter 11, p. 319.
[25] de Boer, B., Stalmach, U., van Hutten, P. F., Melzer, C., Krasnikov, V. V., & Hadziioannou, G. (2001). *Polymer*, *42*, 9097.
[26] Sun, S. (2003). *Sol. Energy Mater. Sol. Cells*, *79*, 257.
[27] Huang, S. Y., Schlichthörl, G., Nozik, A. J., Grätzel, M., & Frank, A. J. (1997). *J. Phys. Chem. B*, *101*, 2576.
[28] Scharber, M. C., Mühlbacher, D., Koppe, M., Denk, P., Waldauf, C., Heeger, A. J., & Brabec, C. J. (2006). *Adv. Mater.*, *18*, 789.
[29] Sun, S., Fan, Z., Wang, Y., & Haliburton, J. (2005). *J. Mater. Sci.*, *40*, 1429.
[30] Knupfer, M. (2003). *Appl. Phys. A*, *77*, 623.
[31] Nishikitani, Y., Kubo, T., & Masuda, H. (2009) MRS Fall Meeting (Boston, USA, 2009/12), *Proceedings*, 1211-R10-03.